JOURNAL OF AGRICULTURAL AND FOOD CHEMISTRY
ARTICLE

J. Agric. Food Chem. 2009, 57, 3867–3876 3867
DOI:10.1021/jf8038956

Introducing Capillary Electrophoresis with Laser-Induced Fluorescence Detection (CE-LIF) for the Characterization of Konjac Glucomannan Oligosaccharides and Their in Vitro Fermentation Behavior

Simone Albrecht, Gonny C. J. van Muiswinkel, Henk A. Schols,*
Alphons G. J. Voragen, and Harry Gruppen

Department of Agrotechnology and Food Sciences, Laboratory of Food Chemistry, Wageningen University, Bomenweg 2, 6703 HD Wageningen, The Netherlands

The application of capillary electrophoresis with laser-induced fluorescence detection (CE-LIF) as a tool for the characterization of complex carbohydrate structures was investigated for konjac glucomannan (KGM) oligosaccharide mixtures and the monitoring of their structural changes during 72 h of in vitro fermentation with human gut flora. Different types of KGM oligosaccharide mixtures were produced from a KGM polysaccharide using endo-β-(1,4)-mannanase and endo-β-(1,4)-glucanase. Distinction of structures emerging from different enzymatic KGM digests and detection of acetylated oligosaccharides were possible by both CE-LIF and matrix-assisted laser desorption/ionization−time-of-flight mass spectrometry (MALDI-TOF MS). Using CE-LIF it could be shown that the endo-β-(1,4)-glucanase digest exhibited a large degradability of the DP2, DP3, DP5, and DP6 components during in vitro fermentation, whereas the endo-β-(1,4)-mannanase digest was digested only slightly, thereby highlighting the influence of structural characteristics on the fermentability by human gut flora.

KEYWORDS: CE-LIF; MALDI-TOF MS; prebiotics; konjac glucomannan oligosaccharides; in vitro fermentation

INTRODUCTION

The profiling of complex oligosaccharides is an analytical challenge, complicated by the presence of numerous isomeric structures. However, the monitoring of structural features of complex carbohydrate substrates during in vitro and in vivo fermentation trials with human gut flora is a crucial step for judging their fate in the human colon and thus their prebiotic potential. Prebiotics are defined to be nondigestible food ingredients that beneficially affect the host by selectively stimulating the growth and/or activity of one or more desired bacteria species in the colon and thus improve host health (*1*). Prebiotics are associated with nondigestible oligosaccharides (NDOs), meaning they are transiting the human small intestine inert (*2*) and, being oligosaccharides, they are defined to consist of 3−10 monosaccharide units according to IUB-IUPAC. However, there is no rational or physiological limit for setting the latter limits of DP10 (*3*). Frequently used prebiotic substrates are lactose-based galacto-oligosaccharides (GOS) and fructo-oligosaccharides (FOS)/inulin, and large numbers of studies have been performed that investigated the prebiotic potential of GOS (*4*) and FOS (*5*), confirming their selective stimulation of beneficial gut bacteria. A drawback of these commonly used prebiotics might be their fast fermentation in the proximal part of the colon (*3*, *6*).

*Author to whom correspondence should be addressed (fax +31 317 484893; telephone +31 317 482239; e-mail henk.schols@wur.nl).

Many colonic diseases, such as ulcerative colitis and tumors, occur in the distal part of the gastrointestinal tract. Targeting the more distal colonic regions is therefore an important issue in the fields of prebiotic research and design (*3*, *7*). Due to their possible resistance to bacterial metabolization in the proximal colon, complex carbohydrate structures are of increasing interest and need to be tested in vitro and in vivo for their prebiotic suitability. Earlier studies on the in vitro fermentability of differently substituted xylo-oligosaccharides (XOS) showed that nonsubstituted XOS were fermented more easily than the more complex structures of acetylated XOS, although the effect of adaption to the substrate has not been described (*8*).

Hence, having a combination of acetylation of the sugars and a backbone of two different sugars, konjac glucomannan (KGM) and oligosaccharides derived thereof seem to be promising prebiotic substrates. KGM is a neutral polysaccharide derived from the tuber of *Amorphophallus konjac* C. Koch and native to Southeast Asia (*9*). It is composed of β-(1,4)-linked D-mannose and D-glucose residues in a molar ratio of 1.6:1 (*10*). Five to ten percent of the hexose residues are acetylated (*11*). However, it has not yet been established if the acetyl groups are attached to the glucose or mannose residues, and our knowledge concerning the sequence of the mannose and glucose residues over the polysaccharidic chain is still limited. Although efforts have been made to investigate the monosaccharide sequence, still blockwise (*12*) as well as

Published on Web 3/18/2009

random distributions (*10*) are being considered. KGM is estimated to be a slightly branched polysaccharide with branches consisting of 11−16 hexose residues (mannose, glucose, and galactose) (*13*).

Besides its potential prebiotic characteristics, KGM is also known to have beneficial effects on human health and has been consumed in Asia for centuries. Being a soluble dietary fiber, it can positively influence hyperglycemia and hypercholesterolemia (*14*, *15*) and may result in a delayed stomach emptying, hence providing a feeling of satiety and possibly facilitating weight loss (*16*).

Studies of the effect of KGM on the fecal microflora in Balb/c mice revealed a dose-dependent bifidogenic effect, especially for hydrolyzed KGM (*17*). However, the influence of fermentation on KGM structures has not yet been studied in detail, mainly due to limited analytical capabilities. Recently, capillary electrophoresis with laser induced fluorescence detection (CE-LIF) has been shown to be a suitable technique for the study of complex oligosaccharide mixtures (*18*, *19*), which are laborious and difficult to analyze using reversed-phase high-performance liquid chromatography (RP-HPLC) (*18*, *19*) or high-performance anion exchange chromatography (HPAEC) (*20*) and mass spectrometry coupling (HPAEC-MS) (*21*). Therefore, in this study CE-LIF and matrix-assisted laser desorption/ionization−time-of-flight mass spectrometry (MALDI-TOF MS) were used to elucidate the structural characteristics and the in vitro fermentation by human gut flora of structurally different KGM oligosaccharide mixtures.

MATERIALS AND METHODS

Materials and Enzymes. The konjac glucomannan polysaccharide (KGM native) was obtained from Kalys (Kalys, St-Ismier, France). The standards used for HPAEC and CE-LIF were cellodextrin [β-(1,4)-linked glucose oligosaccharides] and D-(+)-mannose, both from Sigma-Aldrich (Steinheim, Germany), as well as manno-β-(1,4)-biose, manno-β-(1,4)-triose, manno-β-(1,4)-tetraose, and manno-β-(1,4)-pentaose, all obtained from Megazyme (Bray, Ireland).

The crude cellulase preparation used was produced by *Trichoderma viride* (Maxazyme, DSM Food Specialties, Delft, The Netherlands). Endo-β-glucanase VI [EC 3.2.1.4, GH family 7, specific activity = 11 mU/mg of protein on CM-cellulose (type Akucell AF 0305, Akzo, Arnhem, The Netherlands), 20 mM sodium citrate buffer, pH 3.5, 30 °C] was purified from this commercial cellulase preparation according to the method of Beldman et al. (*22*). Endo-β-mannanase [EC 3.2.1.78, GH family 5, specific activity = 33U/mg of protein on palm kernel mannan (extracted and prepared by Düsterhöft et al. (*23*), 0.05 M sodium acetate buffer, pH 5, 30 °C] was purified from a commercial *Aspergillus niger* enzyme mixture (Gamanase III, Novozymes, Bagsvaerd, Denmark) according to the method of Düsterhöft et al. (*24*).

Preparation of Oligosaccharides from Konjac Glucomannan Polysaccharide. Digestions with the crude cellulase preparation and with the pure endo-β-(1,4)-mannanase were performed in 0.05 M sodium acetate buffer at pH 5. KGM results in highly viscous solutions and tends to form clumps. Therefore, it had to be prepared by adding the KGM powder slowly to vigorously stirred water. The KGM polysaccharide solution (10 mg/mL) was incubated with a 0.1% (v/v) cellulase concentration. The enzyme level applied for endo-β-(1,4)-mannanase was 70 μL of enzyme solution (3.3 U/mL) per milliliter of substrate solution (5 mg/mL). The incubation with endo-β-(1,4)-glucanase VI was performed in 20 mM sodium citrate buffer at pH 3.5, and 363.6 μL of enzyme solution (0.8 U/mL) was added per milliliter of substrate solution (5 mg/mL). The enzyme dosages were chosen according to the best results in oligosaccharide profile obtained after testing different substrate to enzyme ratios. The incubation parameters were 30 °C and 24 h at shaking conditions for all enzymes. After hydrolysis, the enzymes were inactivated (10 min, 100 °C), and the hydrolysate was centrifuged (5 min, 10000*g*, room temperature).

Saponification was performed for 16 h at 4 °C, shaking conditions (25 mL of 0.2 M NaOH per 200 mg of substrate), with parts of the KGM digests to obtain deacetylated material. The solutions were desalted by adding an excess of anion-exchange resin (AG 50W-X8 resin; Bio-Rad, Hercules, CA) and freeze-dried.

For a more detailed structural characterization, the oligosaccharides in the digests were fractionated according to their DP. Fractionation was performed on a Spectra System HPLC (Thermo Finnigan, Waltham, MA) equipped with a Bio-Gel P2 column (1000 × 26 mm, 200−400 mesh, Bio-Rad) thermostated at 60 °C and eluted with Milli-Q water at 0.3 mL/min. Samples (3−13 mg) were either injected by means of an autosampler or directly applied onto the column.

The column efflux was first led through a refractive index detector (Shodex RI72, Showa Denko K.K., Tokyo, Japan) before it was collected in fractions of 10 min by a fraction collector (Superfrac, GE Amersham, Uppsala, Sweden). Appropriate fractions were pooled and freeze-dried for further analysis.

Prior to the fermentation experiment, monomers were removed from the initial KGM digests. The cellulase and endo-β-(1,4)-mannanase digest were subjected to gel filtration on a Superdex 30 prep grade column (600 × 120 mm, 24−49 μm bead size; GE Amersham, Uppsala, Sweden). Samples of up to 2 g were applied on the column and were eluted with distilled water (25 mL/min) at room temperature using an Akta Explorer system (GE Amersham). A Shodex RI-72 detector (Showa Denko K.K.) was used to monitor the refractive index. Fractions were collected each 2 min with a Superfrac fraction collector (GE Amersham) and examined for monomers using HPAEC-PAD. Monomer-free fractions were freeze-dried.

Fermentation. The fermentation broth used was prepared according to the method of Kabel et al. (*8*).

A solution of each konjac glucomannan substrate in water [1% (w/v)] was prepared (S1); for the blank S1 consisted of pure water. The substrates used were fermented in duplicate. For solution 2 (S2) bacto yeast nitrogen base (Difico, Detroit, MI) was dissolved in water (6.7 g/L). Solution 3 (S3) was composed of 40% (v/v) of a watery salt solution [$MgSO_4$ (0.2 g/L), $CaCl_2$ (0.2 g/L), K_2HPO_4 (1 g/L), KH_2PO_4 (1 g/L), $NaHCO_3$ (10 g/L), and NaCl (2 g/L)], 5% (w/v) casein enzymatic hydrolysate (N-Z Amine A, Sigma, St. Louis, MO), and 0.5% (w/v) sodium thioglycolate]. S2 and S3 were adjusted to pH 6−7 by 1 M NaOH. The three solutions S1, S2, and S3 were combined in a ratio of (v/v) 17:1:2 in serum flasks, which were filled at 50% and closed by a butyl rubber stopper. Taking into account Maillard reactions, filter-sterilized S2 was added only after the flasks had been autoclaved (15 min, 121 °C).

To create anaerobic conditions, the air in the serum flasks was exchanged for a N_2 atmosphere (0.7 bar underpressure) by using the Anaerobic Lap system (8 cycles) (GR Instruments B.V., Wijk bij Duurstede, The Netherlands).

Fecal samples were obtained from three healthy human volunteers in sterile plastic cups and were processed shortly after defecation to avoid aerobic conditions. The processing of the samples was performed according to methods of Kabel et al. and Hartemink (*8*, *25*). A 10% (w/v) mixed fecal slurry was prepared by adding one spoon (~5 g) of each fecal sample to 150 mL of buffered peptone water containing L-cysteine−HCl (0.5 g/L, pH 6.7). The fecal slurry was mixed, and after an equilibration time of 30 min, the 10-fold diluted feces were diluted 100 times further by adding them to serum flasks containing a sterilized solution (pH 6.7) of neutralized bacterial peptone (1 g/L), sodium chloride (8 g/L), and L-cysteine−HCl (0.5 g/L) and a N_2 atmosphere.

Serum flasks containing fermentation medium were inoculated with 20% (v/v) of the volume of S1, S2, and S3 present in the flask using the 1000-fold fecal dilutions. The serum flasks,

representing one KGM substrate each, were incubated at 37 °C. Samples were removed eight times between 0 and 72 h. Enzymes were inactivated by heating (5 min, 100 °C, 1100 rpm). The samples were centrifuged, and the supernatants were stored at −80 °C for further analysis.

For a screening of the bacterial growth, the pH of the supernatants was measured, and the optical density of the bacterial residue was determined at 600 nm (GeneQuant pro spectrophotometer, Biochrom, Cambridge, U.K.).

Analytical Methods. *Sugar Composition*. The neutral sugar content and composition were determined by gas−liquid chromatography according to the method of Englyst et al. (*26*) using inositol as an internal standard. Samples were pretreated with aqueous 72% H_2SO_4 (w/w) (1 h, 30 °C), followed by hydrolysis with 1 M H_2SO_4 (3 h, 100 °C) before they were analyzed as volatile alditol acetates on a Carbo Erba Mega 5160 GC (Thermo Finnigan).

Degree of Acetylation (DA). The degree of acetylation was determined according to the method of Voragen et al. (*27*). The ester bonds were saponified by 0.4 N NaOH in a water−isopropanol mixture, and the released acetic acid was determined on a Spectra System HPLC (Thermo Finnigan) equipped with an Aminex HPX 87H column (Bio-Rad) and a Shodex RI72 detector (Showa Denko K.K.). The eluent used was 5.0 mM sulfuric acid (0.6 mL/min, 40 °C).

High Performance Size Exclusion Chromatography. The molecular weight distribution of large oligosaccharide and polysaccharide fractions was investigated by high performance size exclusion chromatography (HPSEC) using a Spectra System HPLC (Thermo Finnigan) equipped with a refractive index detector Shodex RI72 (Showa Denko K.K.). Twenty microliter sample solutions (5 mg/mL) were injected automatically, using a Thermo AS3000 autosampler. Separation was performed on three TosoH Biosep-TSK-Gel G columns in series ($4000PW_{XL}$−$3000PW_{XL}$−$2500PW_{XL}$, each 300 × 7.5 mm; TosoH, Japan) in combination with a PW_{XL} guard column (40 × 6 mm; TosoH). For elution, 0.2 M $NaNO_3$ was used at a flow rate of 0.8 mL/min at 30 °C. The system was calibrated with pullulan standards (Sigma Chemical Co.; mass range from 180 Da to 790 kDa).

MALDI-TOF MS. For MALDI-TOF MS of oligosaccharides, an Ultraflex workstation (Bruker Daltronics, Bremen, Germany) equipped with a nitrogen laser of 337 nm was used. The measurement was performed in the positive mode. After a delayed extraction time of 200 ns, the ions were accelerated with a 25 kV voltage. The data were collected from averaging 100 laser shots, with the lowest laser energy necessary to obtain sufficient spectra intensity.

The mass spectrometer was calibrated with a mixture of maltodextrins (AVEBE, Veendam, The Netherlands; mass range of 527−2309 Da as sodium adducts).

For sample preparation, samples (1 mg/mL) were desalted with anion-exchange material (AG 50W-X8 resin; Bio-Rad). The desalted samples (1 μL) were mixed directely on a MS target plate with 2 μL of matrix solution consisting of a watery solution of 2,5-dihydroxybenzoic acid (10 mg/mL; Bruker Daltonics). The mix was dried under a stream of warm air.

HPAEC. The oligosaccharide profile was monitored by HPAEC (Dionex ISC 3000; Dionex, Sunnyvale, CA), equipped with a Dionex Carbopac PA-1 column (2 × 250 mm) in combination with a Carbopac PA-1 guard column (2 × 50 mm). Samples (20 μL) of a concentration of 0.1 mg/mL were injected by means of a Dionex ISC3000 autosampler. The oligomers were eluted (0.3 mL/min) by using a gradient of 0−400 mM sodium acetate in 100 mM NaOH during 40 min. Each elution was followed by a washing step (5 min, 1 M NaOAc in 100 mM NaOH) and an equilibration step (20 min, 100 mM NaOH). Detection was performed using a Dionex ED40 detector in the pulsed amperometric detection mode.

CE-LIF. Samples for CE-LIF were prepared using the ProteomeLab Carbohydrate Labeling and Analysis Kit (Beckman Coulter, Fullerton, CA). To samples containing approximately 0.1 mg of carbohydrate was added 5 nmol of maltose as an internal standard and mobility marker. This mixture was dried using the SpeedVac Concentrator Savant ISS110 (Thermo Electron Corp., Waltham, MA). The mono- and oligosaccharides present in the dried sample were labeled with 9-aminopyrene-1,4,6-trisulfonate (APTS). Separation of the derivatized carbohydrates was performed using a ProteomeLab PA 800 characterization system (Beckman Coulter) equipped with a polyvinyl alcohol (N−CHO) coated capillary (50 μm × 50.2 cm). Detection was done with a laser-induced fluorescence detector (LIF) (Beckman Coulter) at an excitation wavelength of 488 nm and an emission wavelength of 520 nm after 40 cm capillary length.

The capillary was rinsed with water (5 min, 30 psi) and then with separation gel buffer (2 min, 30 psi); the rinsing buffer was exchanged every 20 samples. Subsequently, samples were loaded hydrodynamically (4 s at 0.5 psi, representing approximately 14 nL of sample solution) on the capillary, which was kept at 25 °C. Separation was performed in the reversed polarity mode (30 kV, 20 min) in a 25 mM sodium acetate buffer (pH 4.75) containing 0.4% polyethylene oxide.

RESULTS

Production and Characterization of KGM Material. Knowledge of the characteristics of KGM material is essential for understanding the changes the material undergoes upon fermentation with human gut flora.

All KGM materials produced were derived from the native polymeric KGM. The sugar composition of the native KGM showed a mannose/glucose molar ratio of 1.5:1 and galactose contributing to the total sugar content with a mole percentage of 1%. The DA was determined to be 7.9%.

For a structural characterization, incubation of the polysaccharide was performed with endo-β-(1,4)-mannanase and endo-β-(1,4)-glucanase.

MALDI-TOF MS was used for a first screening of the KGM oligosaccharides obtained after the enzymatic digestion of the polymer. The mass spectra obtained showed the sodium (Na) and potassium (K) adducts of hexose oligomers. Besides, masses were found that indicate the presence of one to three acetyl groups bound to hexose oligomers. Applying a mass window ranging from m/z 500 to 2500 made it possible to detect oligosaccharides of DP3 to DP14. Monomers, dimers, and oligosaccharides with DP > 14 were not detected with this method.

The use of a purified endo-β-(1,4)-glucanase resulted in the appearance of oligosaccharides covering the whole range of DP3−DP14 (**Figure 1a**). Instead, incubation with endo-β-(1,4)-mannanase resulted in oligosaccharides showing a smaller DP range of DP3−DP9 (**Figure 1b**). Comparison of the MALDI-TOF mass spectra of the endo-β-(1,4)-mannanase digest and the endo-β-(1,4)-glucanase digest revealed a different distribution of acetyl groups on the oligosaccharides with different DPs. The insets in **Figure 1** show the degree of acetyl substitution of the oligosaccharides, based on the signal heights of the MALDI-TOF mass spectra. Within one DP the total height of all Na and K adduct signals was set to 100% and the relative amount of DP having x, y, z, or k acetyl groups was indicated. This is merely an indication, because it was only assumed that all oligomers would have the same response. The higher the DP, the higher seems to be the amount of single-acetylated and multiple-acetylated oligosaccharides for both substrates. The DA of smaller oligomers is higher for the endo-β-(1,4)-mannanase digest.

Because MALDI-TOF MS is only a screening of the oligomers present, another method was needed for a more

detailed characterization. HPAEC-PAD is commonly used for characterizing oligosaccharidic material. Comparison of the HPAEC-PAD separation of the series mannose, mannobiose, and manno-oligosaccharides with the series glucose, cellobiose, and cello-oligosaccharides (**Figure 2a**) revealed a complex elution profile in which elution was certainly not based on size alone. Cellobiose is eluting almost contemporanously with mannopentaose. The mixed glycosidic linkages of glucose and mannose present in KGM make the chromatograms of KGM oligomers even more complex and an assignment of the DPs impossible (data not shown). Therefore, the recently established CE-LIF method was tested for its capacity to separate complex oligomer mixtures resulting from KGM digests. Electrophoretic separation demands charged molecules. Therefore, the neutral oligosaccharides were labeled with the 3-fold negatively charged fluorescent dye APTS. For the standard mixtures a groupwise migration according to the DP was obtained with CE-LIF (**Figure 2b**), which presents a crucial advantage compared to the separation obtained by HPAEC-PAD.

Analyzing the endo-β-(1,4)-mannanase and endo-β-(1,4)-glucanase digests with CE-LIF resulted in electropherograms showing distinct peak clusters with a repeating pattern, especially for the endo-β-(1,4)-glucanase digest (**Figure 3**). Free APTS as well as mono- and oligosaccharidic components of the endo-β-(1,4)-mannanase digest migrated completely between the migration times 3 and 7.5 min, resulting in a separation window of <4.5 min. The peak clusters of the endo-β-(1,4)-glucanase digest were distributed over the whole separation time of 20 min (electropherograms shown were all zoomed in to a maximum of 15 min).

For an identification of the DPs in these complex mixtures of nonacetylated and acetylated oligosaccharides, Biogel P2 fractions of the endo-β-(1,4)-mannanase and endo-β-(1,4)-glucanase digests were analyzed with CE-LIF. The DPs of those fractions were estimated by MALDI-TOF MS. Subsequently, it was possible to assign each of these distinct peak clusters appearing in **Figure 3** with their respective DP. The endo-β(1,4)-mannanase and endo-β-(1,4)-glucanase digest showed complementary peak patterns.

Clearly, CE is able to separate both acetylated and nonacetylated oligosaccharides in a single run, whereas the alkaline HPAEC elution does not give any information on the presence of acetylated oligosaccharides. Saponified substrates were subjected to CE-LIF analysis to investigate if all peaks originally present in electropherograms of nonsaponified substrates were still present after saponification. Peaks that were not present any more were assigned as peaks representing acetylated oligomers. For the endo-β-(1,4)-mannanase digest, disappearance of peaks mainly at the

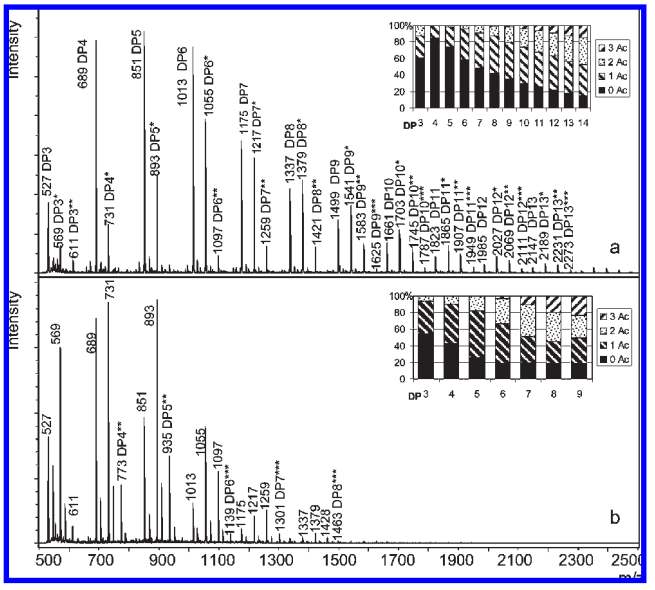

Figure 1. MALDI-TOF mass spectra of (**a**) KGM endo-β-(1,4)-glucanase digest and (**b**) KGM endo-β-(1,4)-mannanase digest. Masses indicated represent sodium adducts. *, Single-acetylated DP; **, double-acetylated DP; ***, triple-acetylated DP. Insets represent the degree of acetylation per DP. (Ac = acetyl group.)

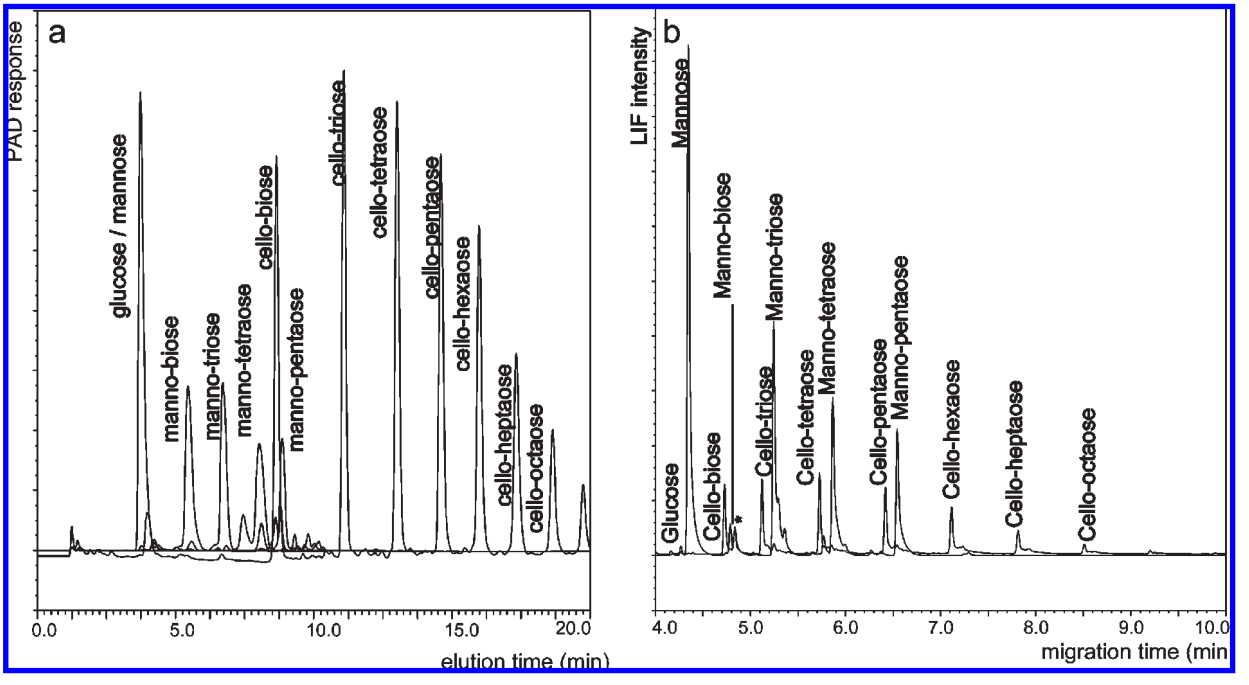

Figure 2. (**a**) HPAEC PAD chromatogram of cello-oligomers and manno-oligomers; (**b**) CE-LIF electropherogram of cello-oligomers and manno-oligomers. *, Maltose (internal standard).

end of each DP cluster was observed (**Figure 4a**), whereas for endo-β-(1,4)-glucanase, the disappearence of peaks was not restricted to the end of the DP clusters (**Figure 4b**). Acetylation is more abundant for higher DPs in the endo-β-(1,4)-glucanase digest, whereas saponification effects already clear changes with DP3 and DP4 in the endo-β-(1,4)-mannanase digest.

In Vitro Fermentation of KGM Material. Because methods were now available for a structural characterization, they were applied to the monitoring of the in vitro fermentation of KGM substrates. Therefore, oligosaccharides were prepared by enzymatic digestion of the KGM polymer with endo-β-(1,4)-mannanase and a crude cellulase mixture.

Four different KGM substrates and a fermentation blank (without any carbohydrate source added) were fermented in duplicate by a fecal slurry consisting of a mix of feces from three human volunteers. In summary, the substrates used were a cellulase and an endo-β-(1,4)-mannanase digest of KGM. The enzymatic digests were used for the fermentation experiments in their monomer-free forms. To test the influence of the presence of monomers, the cellulase digest was as well fermented in its monomer-containing form. The behavior of the KGM oligosaccharides was compared to the fermentation behavior of the parental native polysaccharide KGM.

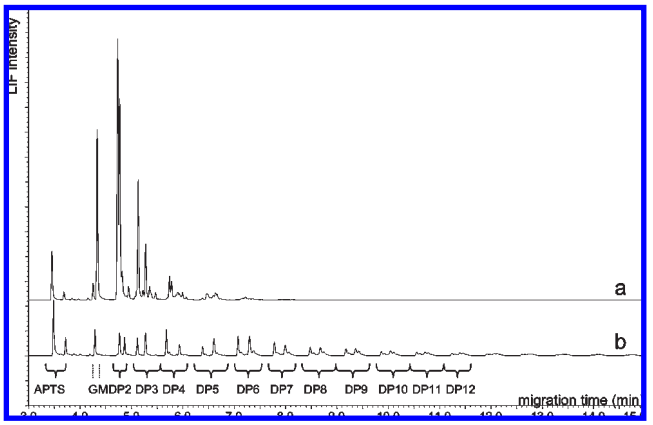

Figure 3. CE-LIF electropherogram of (**a**) KGM endo-β-(1,4)-mannanase digest and (**b**) KGM endo-β-(1,4)-glucanase digest.

The substrates were autoclaved to exclude bacterial contamination. MALDI-TOF mass spectra of autoclaved enzymatically treated KGM material showed largely reduced signal intensity or even a lack of signals for acetylated oligosaccharides. All oligosaccharidic KGM mixtures could, therefore, be considered as substrates low in or without acetyl groups.

For estimating bacterial growth and activity, OD and pH in the samples taken during the fermentation experiment (up to 72 h) were measured. HPSEC, MALDI-TOF MS, and CE-LIF analysis were used to monitor the in vitro fermentation and utilization of the polymer or the individual oligosaccharidic carbohydrate components.

Results from the duplicate experiment were comparable and are not further considered.

All KGM samples showed an increase in optical density and a decrease of pH from an average pH 6.5 to a common end point of pH 4.7−4.8 during 72 h of in vitro fermentation. With the monomer-containing cellulase digest, the pH reached the end point after only 24 h, whereas for the polysaccharide a more gradual decrease to the end point pH after 72 h was found. The result for the monomer-free cellulase digests was situated between these two extrema mentioned. In contrast, the monomer-free endo-β-(1,4)-mannanase digest behaved similarly to the monomer-containing cellulase digests.

The fermentation blank showed neither an increase of OD nor a decrease in pH upon 72 h of fermentation time.

Studying the degradation pattern of the monomer-containing cellulase digest by CE-LIF revealed the following characteristics: Monomeric material was fermented during the first 24 h, and di- and trimers were largely fermented

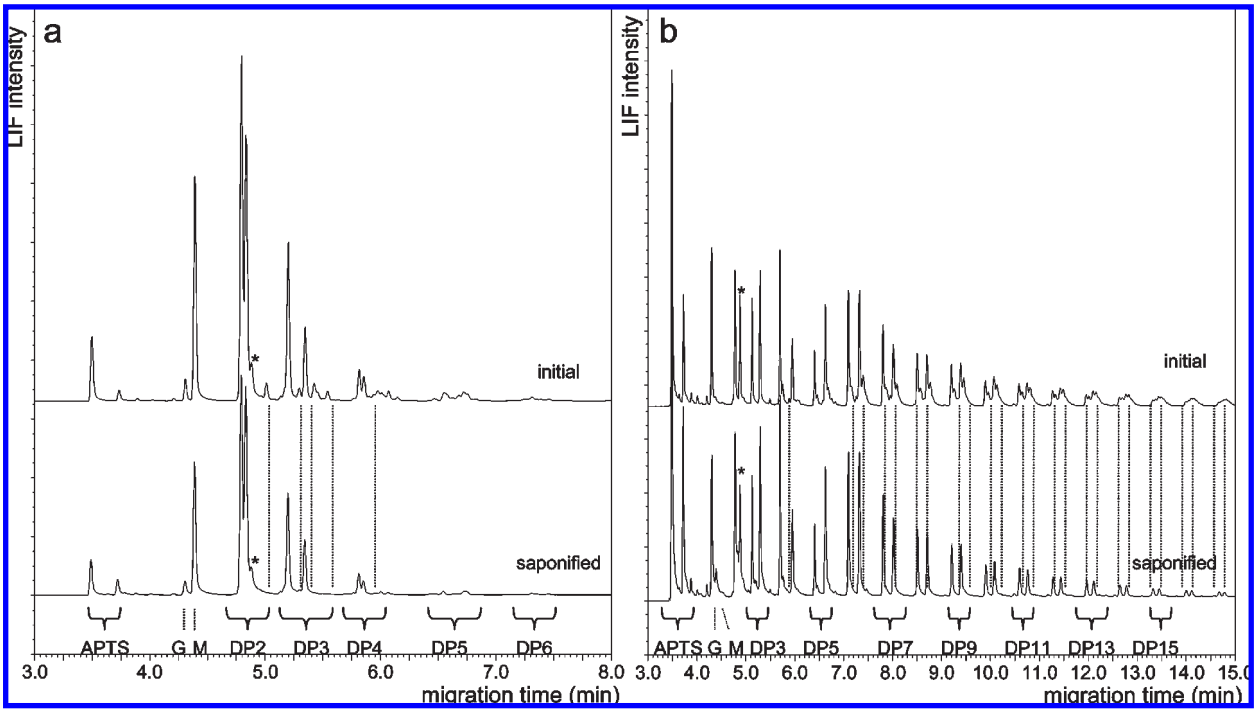

Figure 4. CE-LIF electropherograms of (**a**) initial and saponified KGM endo-β-(1,4)-mannanase digest and (**b**) initial and saponified KGM endo-β-(1,4)-glucanase digest. *, Maltose (internal standard). Vertical dotted lines indicate peaks that are no longer present after the saponification experiment.

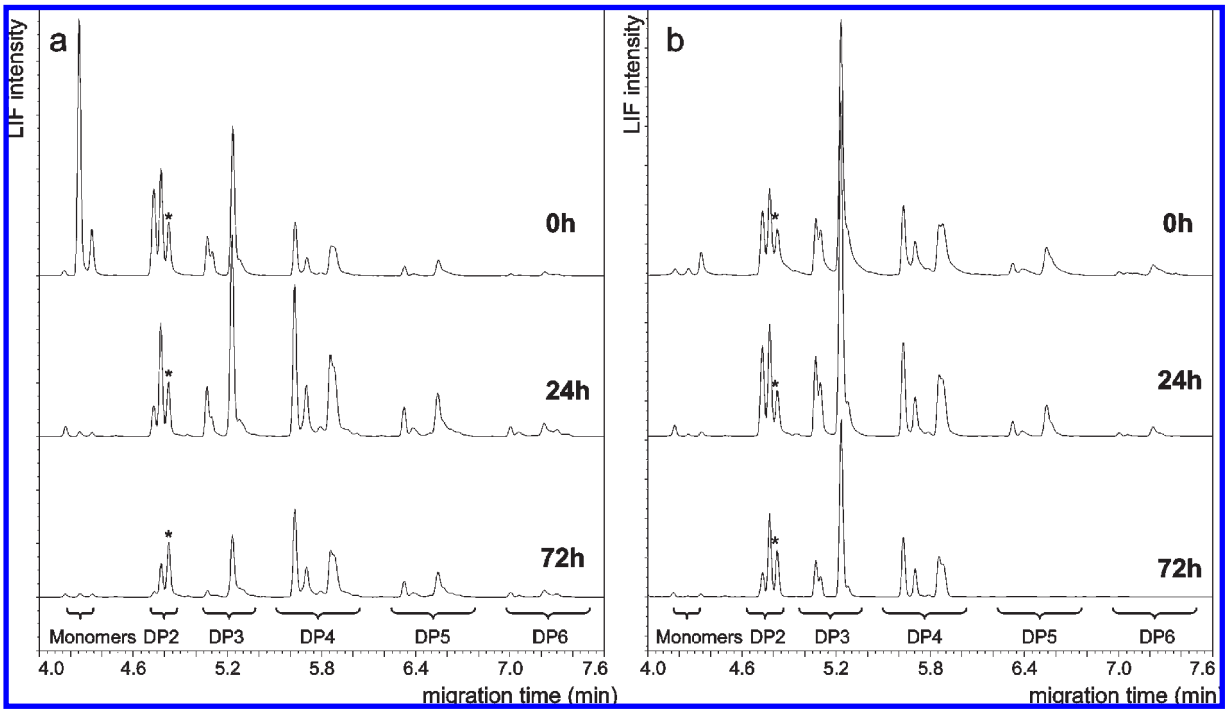

Figure 5. CE-LIF electropherograms obtained after 0, 24, and 72 h of fermentation of (**a**) KGM cellulase digest containing monomers and (**b**) monomer-free KGM cellulase digest. *, Maltose (internal standard).

especially between 24 and 72 h. For the larger oligomers, no changes were observed during the in vitro fermentation (**Figure 5a**).

The fermentation of the monomer-free cellulase digest resulted in a different pattern compared to its monomer-containing analogon (**Figure 5b**). During the first 24 h, no changes within the oligosaccharidic material were observed. Between 24 and 72 h, DP6 was completely and DP5 largely degraded, whereas DP4 was more resistant. The areas of the first peak, identified as a dimer (migration time of 4.7 min), and the peaks belonging to DP3 (migration time between 5.05 and 5.3 min) decreased also over time. The decrease in areas over time for the latter peaks described was 50% higher in the monomer-containing analogue, compared to the monomer-free preparation.

The CE-LIF electropherograms of the cellulase digest at t = 0 h (**Figure 5**) did not completely match with the electropherogram obtained for the endo-β-(1,4)-glucanase digest (**Figure 3b**), as the latter one showed additional side peaks aside from the common main peaks found for both electropherograms.

The CE-LIF electropherograms of the monomer-free endo-β-(1,4)-mannanase digest did not show a distinct degradation pattern. The increase of oligosaccharides with the size of DP3 indicated, nevertheless, an ongoing carbohydrate fermentation upon 72 h of fermentation.

MALDI-TOF MS results of the KGM mixtures confirmed the degradation of oligosaccharidic material during the 72 h in vitro fermentation and did not provide any further information.

Analysis of CE-LIF electropherograms, MALDI-TOF mass spectra, and HPSEC chromatograms resulted in complementary information concerning the fermentation of the KGM polymer. As observed by the shift in molecular weight in **Figure 6a**, the polymer, which had originally a M_w of ≥500 000 (≥DP 3000), was gradually degraded to oligomeric material during 72 h of fermentation. By integrating the areas under the curves it could be stated that the oligomers formed were also utilized to some extent. The peak areas representing oligomeric material increased to only 35% of the decreased area belonging to polymeric material in the HPSEC chromatograms. In **Figure 6b**, the emergence of oligomers during the fermentation of the polymer is shown by CE-LIF electropherograms. The intensity of the oligomers increased, with DP5 being the most abundant DP after 72 h. MALDI-TOF mass spectra showed, in addition to the emerging series of hexoses, the appearances of series of masses representing single-acetylated hexoses.

DISCUSSION

Characterization of KGM Material. To study the influence of the chemical structure and the KGM mixture composition on the fermentability, the KGM material used for fermentation was characterized in the first part of this study. Combination of MALDI-TOF MS with results obtained by applying the recently established CE-LIF method contributed to a structural approach on endo-β-mannanase and endo-β-(1,4)-glucanase digests of KGM.

For KGM with a M/G ratio of 1.5:1, the KGM chain provided more cleaving sites for an enzymatic digest with endo-β-(1,4)-mannanase, which is expected to cleave the glycosidic linkage between two mannose residues (DP3−DP9 in MALDI-TOF mass spectra) than for an enzymatic digest with endo-β-(1,4)-glucanase, which is expected to cleave the glycosidic linkage between two glucose residues (DP3−DP14 in MALDI-TOF mass spectra). Not only the excess of mannose residues in the KGM polysaccharide but also the fact that endo-β-(1,4)-mannanases cleave M−G bonds in the konjac glucomannan polysaccharidic chain (*28*) explains the good degradability of KGM with endo-β-(1,4)-mannanase as observed with MALDI-TOF MS.

The enhanced degradation with endo-β-(1,4)-mannanase was confirmed with CE-LIF, which provided oligosaccharide

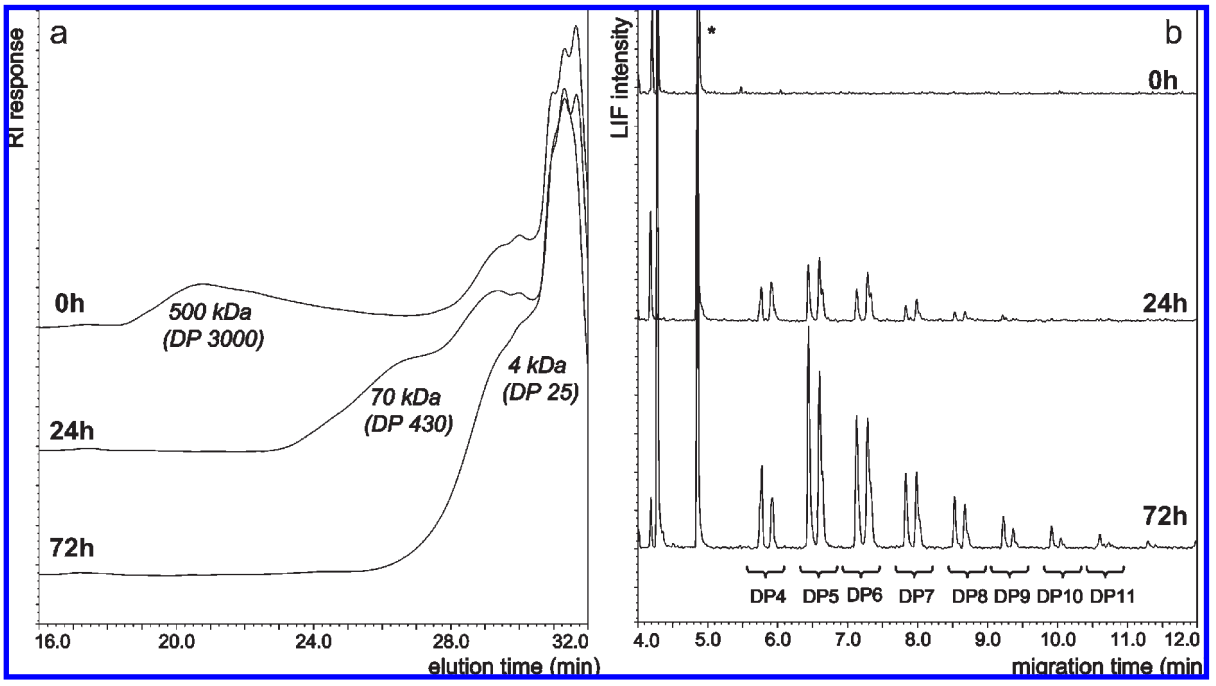

Figure 6. (**a**) HPSEC chromatograms obtained after 0, 24, and 72 h of fermentation of the KGM polysaccharide; (**b**) CE-LIF electropherograms obtained after 0, 24, and 72 h of fermentation of the KGM polysaccharide. *, Maltose (internal standard).

separation that showed advantages over the commonly performed separation with HPAEC-PAD and can be considered as the method of choice for the structural analysis of complex carbohydrate oligosaccharides. Besides the fast separation (20 min per run), the mole-based detection, and the detection of acetylated oligosaccharides, a distinct separation in peak clusters representing oligosaccharides of the same DP was obtained with CE-LIF. A complementary structural composition was found for the endo-β-(1,4)-mannanase and the endo-β-(1,4)-glucanase digests of KGM. Saponification experiments resulted in the detection of acetylated oligosaccharides that differed in position in the electropherograms of the endo-β-(1,4)-mannanase and endo-β-(1,4)-glucanase digest. The results obtained for the saponification experiment with CE-LIF analysis (**Figure 4**) have to be compared with the results found for the acetylation pattern with MALDI-TOF MS (**Figure 1**). Both digests showed an increased intensity for acetylated oligosaccharides with increasing DP in their mass spectra as well as in their electropherograms. However, the endo-β-(1,4)-glucanase digest showed a lower release of acetylated oligosaccharides for DP2−DP4. The endo-β-(1,4)-glucanase is therefore assumed to be less tolerant toward acetylation in the glucomannan backbone.

Hypothesizing the Chemical Structure of KGM. By combining results, it was possible to form a hypothesis on the chemical structure. Peak assignment was done by transferring information given by Cescutti et al. (*10*), who examined enzymatic digests of KGM produced by endo-β-(1,4)-mannanase (issuing from *A. niger*) and cellulase (issuing from *Penicillum funiculosum*) with CE and ^{1}H NMR spectroscopy. Additionally, the migration profile of oligosaccharide standards consisting of β-linked glucose or mannose moieties was considered. The action pattern of an enzyme is highly dependent on its origin as well as the sugar composition of the substrate (*29*). Threfore, the action pattern of the endo-β-(1,4)-glucanase and endo-β-(1,4)-mannanase used can be the easiest verified by evaluating the dimers formed by these two enzymes (**Figure 7a**). The endo-β-(1,4)-glucanase digest resulted in one dimer only, which did not migrate at the same time as either the cellobiose standard (GG; migration time of standard GG is indicated as ** in **Figure 7a**; G stands for glucose) or the mannobiose standard (MM; migration time of standard MM is indicated as *** in **Figure 7a**; M stands for mannose). The peak was identified as MG, as endo-β-(1,4)-glucanases are not supposed to cleave glycosidic linkage after mannose residues, but it showed clearly that the endo-β-(1,4)-glucanase used is capable of cleaving the linkage between glucose and mannose residues. For the endo-β-(1,4)-mannanase digest, two dimers were identified, of which one could be identified as MM. The earlier-migrating dimer was assigned as GM, having a slightly later migration time than the dimer assigned as MG in the endo-β-(1,4)-glucanase digest, and explains the capability of the endo-β-mannanas used to cleave linkages between mannose and glucose.

Within each DP, standards composed of glucose units migrated earlier than standards composed of mannose units (**Figure 2b**). On the basis of the latter fact, each peak cluster representing one DP in the KGM digests was divided into two subgroups, as demonstrated for DP3 in **Figure 7b**. According to the migration profile of the references, the subgroup migrating earlier (subgroup I) was assigned to be the one richer in glucose (migration time of standard GGG is indicated as $^{++}$ in **Figure 7b**), whereas the subgroup migrating later (subgroup II) was assigned to be the one richer in mannose (migration time of standard MMM is indicated as $^{+++}$ in **Figure 7b**). A hypothesis on the structures was formed on the basis of the relative concentrations of trimeric structures as identified by Cescutti et al. (*10*). For the endo-β-(1,4)-mannanase digest GGM and GMM were reported to occur in a ratio of 1.00:0.52. Therefore, the peak in subgroup I was assigned as GGM and the most abundant peak in subgroup II as GMM. Also, MMM was identified in subgroup II by its respective standard and was, as well as MGM, reported to be a minor component of the trimeric fraction (*10*). However, no peak was assigned to MGM in the

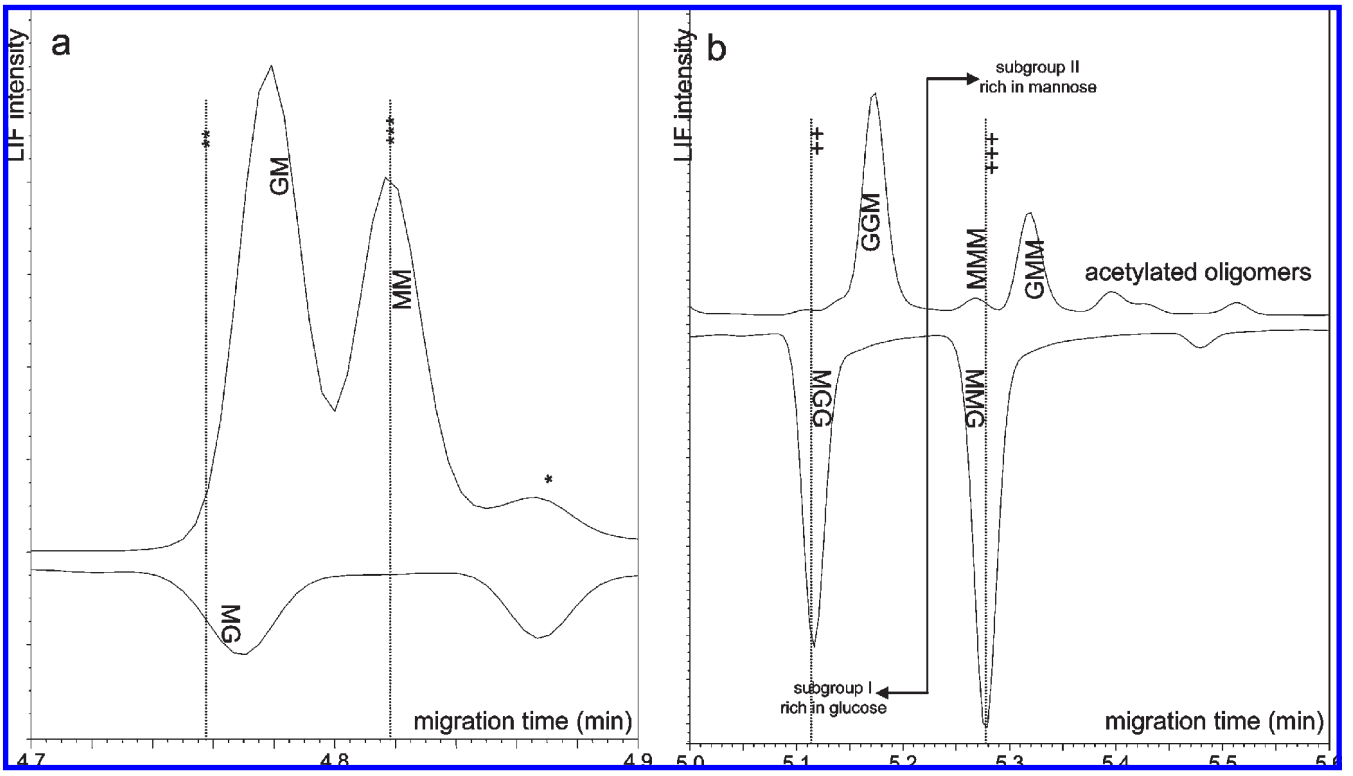

Figure 7. Hypothesis on the structure of KGM; CE-LIF electropherograms of mirrored zoom-ins of **Figure 3** for the KGM endo-β-(1,4)-mannanase digest (normal view) and endo-β-(1,4)-glucanase digest (mirrored view) for (**a**) DP2 and (**b**) DP3. *, Maltose (internal standard); $^{++}$/**, migration time of GG/GGG standard, respectively; $^{+++}$/***, migration time of MM/MMM standard, respectively.

electropherogram. Comigration was assumed. Due to the saponification trials performed, peaks migrating later than GMM were assigned to acetylated trimers. Having used a cellulase preparation, the information given by Cescutti et al. (MMG/MMM/MGG 1.83:1.00:0.2) (*10*) was not completely adaptable to the digestion with endo-β-(1,4)-glucanase performed in the present study. Neglecting the formation of MMM, which is, considering the formation of dimers, not probable to occur by using this pure endo-β-(1,4)-glucanase, the two trimers were assigned for MGG in subgroup I and MMG in subgroup II.

This structural characterization confirmed the action expected for the enzymes applied and justified the assumption of a clustered migration according to the predominance of glucose or mannose in the oligomers. Oligomers found in the endo-β-(1,4)-glucanase digest were assigned to carry exclusively glucose residues at the reducing end, revealing that endo-β-(1,4)-glucanases are not able to cleave the frequently occurring mannotri, -tetra, and -pentaose segments present in the KGM polymer chain (*30*). On the other hand, oligomers found in the endo-β-(1,4)-mannanase digest were assigned to carry exclusively mannose residues at the reducing end but predominantly glucose residues at the nonreducing end. Similar observations were made by Shimahara et al. (*28*, *31*). The repeating peak pattern obtained in the electropherograms [especially for the endo-β-(1,4)-glucanase digest] supports the block model for the KGM polymer instead of a random distribution of glucose and mannose residues. However, the higher the DP, the more peaks remain unknown, due to the increasing complexity of the KGM oligosaccharides and possible comigrations.

From the literature, it is not known on which sugar residue acetyl groups are preferably situated in KGM. However, as acetylation intensity is increasing for the higher MW oligosaccharides in the endo-β-(1,4)-glucanase digest, which are assumed to be especially rich in mannose, it can be assumed that the acetyl groups are preferably attached to the mannose residues. Furthermore, saponification of endo-β-(1,4)-mannanase digests resulted in a preferred disappearance of peaks belonging to subgroup II, representing oligosaccharides richer in mannose. The investigations made for the acetylation of a glucomannan from *Lupinus varius* seed (*32*) showed as well acetylation of the mannose residues in the glucomannan chain.

In Vitro Fermentation of KGM Material. In the second part of this study, native KGM and oligosaccharide mixtures representing cellulase and endo-β-(1,4)-mannanase digests of KGM were successfully fermented by mixed fecal slurries.

Autoclaving the substrates before fermentation significantly decreased the level of acetylation. Autoclaving should be replaced by another sterilization method (e.g., based on filtration) in subsequent fermentation studies. However, choosing a sterilization method based on filtration may be difficult to apply for viscous polysaccharides such as KGM.

During the fermentation course of 72 h, different degradation patterns for the respective KGM substrates were observed.

Due to the use of a cellulase preparation instead of a pure endo-β-(1,4)-glucanase, the initial peak pattern on CE-LIF showed additional side peaks for the cellulase digest, which can be explained by the presence of endo-β-(1,4)-glucanases as well as exo-β-(1,4)-glucosidases in the cellulase preparation used (*22*). With the monomer-containing cellulase digest, a complete utilization of the abundant amount of monomers occurred during the first 24 h. Dimers and trimers were largely degraded, and oligosaccharides of DP4−DP6 did not change upon 72 h of fermentation. Monomers effect the inhibition of enzymes responsible for degrading

oligosaccharides of higher M_w and promote the prevalence of certain species. The promotion of lactic acid bacteria (esp. *Streptococcus* species) by monomeric material and the simultaneous suppression of *Bacteroides* and *Bifidobacteria* species have been reported by Olano-Martin et al. (*33*) and explain the rapid drop in pH during the first 24 h of fermentation.

For the monomer-free cellulase digest, differences in the degradation pattern were observed when compared to the monomer-containing analogue. This emphasizes the necessity of removing monomers before fermentation experiments, as they are also absorbed in the upper gastrointestinal tract and do not reach the colon. Besides the degradation of DP2 and DP3 a degradation of oligomers ≥DP5 was observed after an adaption time of 24 h. DP4 was more resistant to fermentation. Comparable to that, Kabel et al. (*8*) found a preferential fermentation of low substituted acetylated xylo-oligosaccharide with a DP of 3 and a DP >7.

The lack of easily accessible material in the monomer-free cellulase digest stimulated the development of an environment having other bacterial enzymes and/or even bacterial species present, which are responsible for the degradation of higher M_w oligomers. The contribution of a broader range of bacteria may explain the less pronounced decrease in pH during the first 24 h (pH ≥5). Nevertheless, a final pH of 4.6 was reached after 24 h, which is suitable for a suppression of pathogenic species (*1*).

According to the mass spectra and electropherograms, there was hardly any change in the carbohydrate profile during the 72 h fermentation course of the monomer-free KGM endo-β-(1,4)-mannanase digest. The large pH drop and increase in OD during the first 24 h pointed nevertheless to an ongoing degradation, most probably consisting of a utilization of low-M_w material hidden by a meanwhile degradation of high-M_w oligomers out of the range of detection by MALDI-TOF MS and CE-LIF. The structural composition has obviously a big influence on the fermentation behavior: studying the structure of the endo-β-(1,4)-mannanase digest led to the conclusion that glucose or cellobiose is most frequently situated at the nonreducing end. For the cellulase digests it was assumed to be mainly mannose. Consequently, by the activity of bacterial exoenzymes, another set of mono- and dimers is provided for bacterial metabolization. High amounts of released glucose and therefore a predominance of lactic acid bacteria are as well indicated by the rapid drop in pH during the first 24 h of the fermentation of the endo-β-(1,4)-mannanase digest, which is similar to the behavior observed for the monomer-containing cellulase digest.

The fermentation of the parental polysaccharide was monitored by HPSEC, which showed the gradual degradation of the polymer (~500 kDa) to an oligosaccharide mixture (≤4 kDa) after 72 h. Emerging oligomers were characterized by MALDI-TOF MS and CE-LIF. The peak profile in the electropherograms, of which each DP cluster could be subdivided into two subgroups again, did not match exclusively with the profile of one of the enzymatic digests but was a combination of both, indicating the action of a broad range of endo- and exoenzymes expressed in the human colonic flora in order to break down a complex polysaccharide. The pH decreased very gradually and was still ≥5 after 24 h. As was described by Van Laere et al. (*34*), the degradation of a polymer is a synergistic action, resulting in the expression of a broad variety of enzymes and bacteria.

Our study showed that the availability of advanced analytical methods is crucial for monitoring and understanding the behavior of complex carbohydrate structures during their in vitro fermentation. Structural features, composition, and method of preparation of the KGM mixtures had a large influence on the respective fermentation with human fecal flora.

Combining results obtained from fermentation studies is necessary for a good understanding of bacterial action. Therefore, the inclusion of the online CE-LIF-MS coupling, allowing the assignment of peaks present in CE-LIF electropherograms with their respective masses, is aimed for. Furthermore, biomolecular methods such as Polymerase Chain Reaction−Denaturing Gradient Gel Electrophoresis (PCR-DGGE), a method used for investigating complex bacterial communities, and quantitative PCR, with which it is possible to establish a prebiotic index for potential prebiotic substrates, are currently applied for in vitro fermented konjac glucomannan substrates in our laboratory. The determination of the bacterial metabolization products (organic acids) with GC and GC-MS will be our further approach to completely understand the fate of prebiotic substrates subjected to human gut flora.

Although in vitro fermentation experiments do not allow a precise prediction of the fermentation in vivo (lack of buffered gut environment, strict anaerobicity and influence of other food components, adaptation of the flora subjected to prolonged exposure to specific prebiotic, strong influence of chosen concentrations of substrate to inoculum in in vitro experiments), they show clearly that the structural modification of oligosaccharides presents an effective way to influence the microbial community in the gut.

LITERATURE CITED

(1) Gibson, G. R.; Roberfroid, M. B. Dietary modulation of the human colonic microbiota: introducing the concept of prebiotics. *J. Nutr.* **1995**, No. 125, 1401–1412.

(2) Asp, N.-G. Dietary carbohydrates: classification by chemistry and physiology. *Food Chem.* **1996**, *57*, 9–14.

(3) Voragen, A. G. J. Technological aspects of functional food-related carbohydrates. *Trends Food Sci. Technol.* **1998**, *9*, 328.

(4) Ito, M.; Deguchi, Y.; Matsumoto, K.; Kimura, M.; Onodera, N.; Yajima, T. Influence of galactooligosaccharides on the human fecal microflora. *J. Nutr. Sci. Vitaminol.* **1993**, *39*, 635–640.

(5) Wang, X.; Gibson, G. R. Effects of the *in vitro* fermentation of oligofructose and inulin by bacteria growing in the human large intestine. *J. Appl. Bacteriol.* **1993**, *75*, 373–380.

(6) Macfarlane, G. T.; Gibson, G. R.; Cummings, J. H. Comparison of fermentation reactions in different regions of the human colon. *J. Appl. Bacteriol.* **1992**, *72*, 57–64.

(7) Gibson, G. R.; Probert, H. M.; van Loo, J.; Rastall, R. A.; Roberfroid, M. B. Dietary modulation of the human colonic microbiota: updating the concept of prebiotics. *Nutr. Res. Rev.* **2004**, *17*, 259–275.

(8) Kabel, M. A.; Kortenoeven, L.; Schols, H. A.; Voragen, A. G. J. In vitro fermentability of differently substituted xylo-oligosaccharides. *J. Agric. Food Chem.* **2002**, *50*, 6205–6210.

(9) Takigami, S. Konjac mannan. In *Handbook of Hydrocolloids*; Phillips, G. O., Williams, P. A., Eds.; Woodhead Publishing: Cambridge, U.K., 2000; pp 413−423.

(10) Cescutti, P. P.; Campa, C. C.; Delben, F. F.; Rizzo, R. R. Structure of the oligomers obtained by enzymatic hydrolysis of the glucomannan produced by the plant *Amorphophallus konjac*. *Carbohydr. Res.* **2002**, *337*, 2505.

(11) Maekaji, K. Determination of acidic component of konjac mannan. *Agric. Biol. Chem.* **1978**, *42*, 177–178.

(12) Katsuraya, K.; Okuyama, K.; Hatanaka, K.; Oshima, R.; Sato, T.; Matsuzaki, K. Constitution of konjac glucomannan: chemical analysis and ^{13}C NMR spectroscopy. *Carbohydr. Polym*. **2003**, *53*, 183.
(13) Stephen, A. M. Other plant polysaccharides. In *The Polysaccharides*; Aspinall, G. O., Ed.; Academic Press: New York, 1983; Vol. *2*, pp 97−192.
(14) Vuksan, V.; Jenkins, D. J.; Spadafora, P.; Sievenpiper, J. L.; Owen, R.; Vidgen, E.; Brighenti, F.; Josse, R.; Leiter, L. A.; Bruce-Thompson, C. Konjac-mannan (glucomannan) improves glycemia and other associated risk factors for coronary heart disease in type 2 diabetes. A randomized controlled metabolic trial. *Diabetes Care* **1999**, *22*, 913–919.
(15) Wu, J. J.; Peng, S. S. Comparison of hypolipidemic effect of refined konjac meal with several common dietary fibers and their mechanisms of action. *Biomed. Environ. Sci*. **1997**, *10*, 27–37.
(16) Walsh, D. E.; Yaghoubian, V.; Behforooz, A. Effect of glucomannan on obese patients: a clinical study. *Int. J. Obes*. **1984**, *8*, 289–293.
(17) Chen, H. L.; Fan, Y. H.; Chen, M. E.; Chan, Y. Unhydrolyzed and hydrolyzed konjac glucomannans modulated cecal and fecal microflora in Balb/c mice. *Nutrition* **2005**, *21*, 1059–1064.
(18) Hilz, H.; de Jong, L. E.; Kabel, M. A.; Schols, H. A.; Voragen, A. G. J. A comparison of liquid chromatography, capillary electrophoresis, and mass spectrometry methods to determine xyloglucan structures in black currants. *J. Chromatogr., A* **2006**, *1133*, 275–286.
(19) Kabel, M. A.; Heijnis, W. H.; Bakx, E. J.; Kuijpers, R.; Voragen, A. G. J.; Schols, H. A. Capillary electrophoresis fingerprinting, quantification and mass-identification of various 9-aminopyrene-1,4,6-trisulfonate-derivatized oligomers derived from plant polysaccharides. *J. Chromatogr., A* **2006**, *1137*, 119–126.
(20) Lee, Y. Y. C. Carbohydrate analyses with high-performance anion-exchange chromatography. *J. Chromatogr., A* **1996**, *720*, 137–149.
(21) Schols, H. A.; Kabel, M. A.; Bakx, E. J.; Daas, P. J. H.; Alebeek, G.-J.; Voragen, A. G. J. HPLC of oligosaccharides: new developments in detection and peak identification. In *AVH Association—7th Symposium;* Comptes Rendus: Reims, France, 2000; 39−45.
(22) Beldman, G.; Searlevanleeuwen, M. F.; Rombouts, F. M.; Voragen, A. G. J. The cellulase of *Trichoderma viride*—purification, characterization and comparison of all detectable endoglucanases, exoglucanases and β-glucosidases. *Eur. J. Biochem*. **1985**, *146*, 301–308.
(23) Düsterhöft, E.-M.; Posthumus, M. A.; Voragen, A. G. J. Non-starch polysaccharides from sunflower (*Helianthus annuus*) meal and palm-kernel (*Elaeis guineensis*) meal—investigation of the structure of major polysaccharides. *J. Sci. Food Agric*. **1992**, *59*, 151–160.
(24) Düsterhöft, E.-M.; Bonte, A. W.; Voragen, A. G. J. Solubilisation of non-starch polysaccharides from oil-seed meals by polysaccharide-degrading enzymes. *J. Sci. Food Agric*. **1993**, *63*, 211–220.
(25) Hartemink, R. *Prebiotic effects of non-digestible oligo- and poysaccharides*. Ph.D. thesis, Food Microbiology, Wageningen University, The Netherlands, 1999.
(26) Englyst, H.; Wiggins, H. S.; Cummings, J. H. Determination of the non-starch polysaccharides in plant foods by gas−liquid-chromatography of constituent sugars as alditol acetates. *Analyst* **1982**, *107*, 307–318.
(27) Voragen, A. G. J.; Schols, H. A.; Pilnik, W. Determination of the degree of methylation and acetylation of pectins of HPLC. *Food Hydrocolloids* **1986**, *1*, 65–70.
(28) Shimahara, H.; Suzuki, H.; Sugiyama, N.; Nishizawa, K. Isolation and characterization of oligosaccharides from an enzymatic hydrolyzate of konjac mannan. *Agric. Biol. Chem*. **1975**, *39*, 293–299.
(29) Tenkanen, M.; Makkonen, M.; Perttula, M.; Viikari, L.; Teleman, A. Action of *Trichoderma reesei* mannanase on galactoglucomannan in pine kraft pulp. *J. Biotechnol*. **1997**, *57*, 191–204.
(30) Biely, P.; Tenkanen, M. Enzymology of hemicellulose degradation. In *Trichoderma and Gliocladium*; Kubicek, C. P., Harman, G.-E., Ondik, K.-L., Eds.; Taylor and Francis: London, U.K., 1998; Vol. *2*, pp 25−47.
(31) Shimahara, H.; Suzuki, H.; Sugiyama, N.; Nisizawa, K. Partial purification of β-mannanases from the konjac tubers and their substrate specifity in the relation to the structure of konjac glucomannan. *Agric. Biol. Chem*. **1975**, *39*, 301–312.
(32) Ishurd, O.; Kermagi, A.; Elghazoun, M.; Kennedy, J. F. Structural of a glucomannan from *Lupinus varius* seed. *Carbohydr. Polym*. **2006**, *65*, 410–413.
(33) Olano-Martin, E.; Gibson, G. R.; Rastall, R. A. Comparison of the *in vitro* bifidogenic properties of pectins and pectic-oligosaccharides. *J. Appl. Microbiol*. **2002**, *93*, 505–511.
(34) Van Laere, K. M. J.; Hartemink, R.; Bosveld, M.; Schols, H. A.; Voragen, A. G. J. Fermentation of plant cell wall derived polysaccharides and their corresponding oligosaccharides by intestinal bacteria. *J. Agric. Food Chem*. **2000**, *48*, 1644–1652.

Received for Review December 16, 2008. Accepted March 06, 2009. Revised manuscript received February 25, 2009.